Stem Cell Reports
Article
ISSCR
OPEN ACCESS

# Maternal Western-style diet remodels the transcriptional landscape of fetal hematopoietic stem and progenitor cells in rhesus macaques

Suhas Sureshchandra,[1] Chi N. Chan,[2] Jacob J. Robino,[3] Lindsay K. Parmelee,[2] Michael J. Nash,[4] Stephanie R. Wesolowski,[4] Eric M. Pietras,[5] Jacob E. Friedman,[4,6] Diana Takahashi,[2] Weining Shen,[7] Xiwen Jiang,[7] Jon D. Hennebold,[8,9] Devorah Goldman,[10] William Packwood,[11] Jonathan R. Lindner,[3,11] Charles T. Roberts, Jr.,[3,12] Benjamin J. Burwitz,[13,14] Ilhem Messaoudi,[1,15] and Oleg Varlamov[3,*]

[1]Department of Molecular Biology and Biochemistry, School of Biological Sciences, Institute for Immunology, Center for Virus Research, University of California-Irvine, Irvine, CA 92697, USA
[2]Division of Comparative Medicine, Oregon National Primate Research Center, Beaverton, OR 97006
[3]Division of Cardiometabolic Health, Oregon National Primate Research Center, Beaverton, OR 97006
[4]Department of Pediatrics, Section of Neonatology, University of Colorado Anschutz Medical Campus, Aurora, CO 80045, USA
[5]Department of Immunology and Microbiology, Division of Hematology, University of Colorado Anschutz Medical Campus, Aurora, CO 80045, USA
[6]Harold Hamm Diabetes Center, University of Oklahoma Health Sciences Center, Oklahoma City, OK 73104, USA
[7]Department of Statistics, University of California-Irvine, Irvine, CA 92697, USA
[8]Division of Reproductive and Developmental Sciences, Oregon National Primate Research Center, Beaverton, OR 97006
[9]Department of Obstetrics and Gynecology, Oregon Health & Science University, Portland, OR 97239, USA
[10]Stem Cell Center, Oregon Health & Science University, Portland, OR 97239, USA
[11]Knight Cardiovascular Institute, Oregon Health & Science University, Portland, OR 97239, USA
[12]Department of Pediatrics, Oregon Health & Science University, Portland, OR 97239, USA
[13]Division of Pathobiology and Immunology, Oregon National Primate Research Center, Beaverton, OR 97006
[14]Vaccine & Gene Therapy Institute, Beaverton, OR 97006, USA
[15]Department of Immunology, Microbiology and Molecular Genetics, University of Kentucky College of Medicine, Lexington, KY 40506, USA
*Correspondence: varlamov@ohsu.edu
https://doi.org/10.1016/j.stemcr.2022.10.003

## SUMMARY

Maternal obesity adversely impacts the *in utero* metabolic environment, but its effect on fetal hematopoiesis remains incompletely understood. During late development, the fetal bone marrow (FBM) becomes the major site where macrophages and B lymphocytes are produced via differentiation of hematopoietic stem and progenitor cells (HSPCs). Here, we analyzed the transcriptional landscape of FBM HSPCs at single-cell resolution in fetal macaques exposed to a maternal high-fat Western-style diet (WSD) or a low-fat control diet. We demonstrate that maternal WSD induces a proinflammatory response in FBM HSPCs and fetal macrophages. In addition, maternal WSD consumption suppresses the expression of B cell development genes and decreases the frequency of FBM B cells. Finally, maternal WSD leads to poor engraftment of fetal HSPCs in nonlethally irradiated immunodeficient NOD/SCID/*IL2rγ*$^{-/-}$ mice. Collectively, these data demonstrate for the first time that maternal WSD impairs fetal HSPC differentiation and function in a translationally relevant nonhuman primate model.

## INTRODUCTION

Pre-pregnancy obesity is associated with increased risk of infection (Rastogi et al., 2015; Suk et al., 2016) and aberrant inflammatory responses (Kamimae-Lanning et al., 2015; Odaka et al., 2010) in the offspring. However, there is a paucity of studies that examine the impacts of maternal obesity on fetal hematopoiesis in models that resemble human development. Hematopoiesis occurs in several waves that involve the migration of hematopoietic stem and progenitor cells (HSPCs) between different hematopoietic sites (Gao et al., 2018). Following the emergence of HSPCs in the aorta-gonad-mesonephros during the first trimester, the fetal liver (FL) becomes the main hematopoietic niche for HSPC expansion (Bowie et al., 2007; Morrison et al., 1995). During the second and third trimesters, HSPCs migrate from the FL to the fetal bone marrow (FBM) (Christensen et al., 2004; Coskun et al., 2014), where monocyte-derived macrophages and B lymphocytes are produced throughout life (Gomez Perdiguero et al., 2015; McGrath et al., 2015; Orkin and Zon, 2008). Both monocytes and tissue-resident macrophages are important for anti-microbial defense (Gomez Perdiguero et al., 2015). Therefore, alterations in the maternal environment may affect offspring immunity by reprogramming HSPC outputs in the FBM and the FL (Friedman, 2018); however, the molecular mechanisms responsible remain poorly understood. In the present study, we investigated these mechanisms by leveraging a rhesus macaque model, whose hematopoietic (Kim et al., 2014; Larochelle et al., 2011; Lee et al., 2005; Radtke et al., 2019; Sykes and Scadden, 2013; Varlamov et al., 2020; Wu et al., 2018) and immune (Batchelder et al., 2014; Messaoudi et al., 2011; Tarantal et al., 2022) systems are highly similar to that of humans. Female macaques were exposed to a high-fat Western-style diet (WSD) or low-fat monkey chow (control diet) beginning at puberty (True et al., 2017). After 5.5 years of treatment, animals underwent timed mating breeding. To reduce the


This is an open access article under the CC BY-NC-ND license (http://creativecommons.org/licenses/by-nc-nd/4.0/).

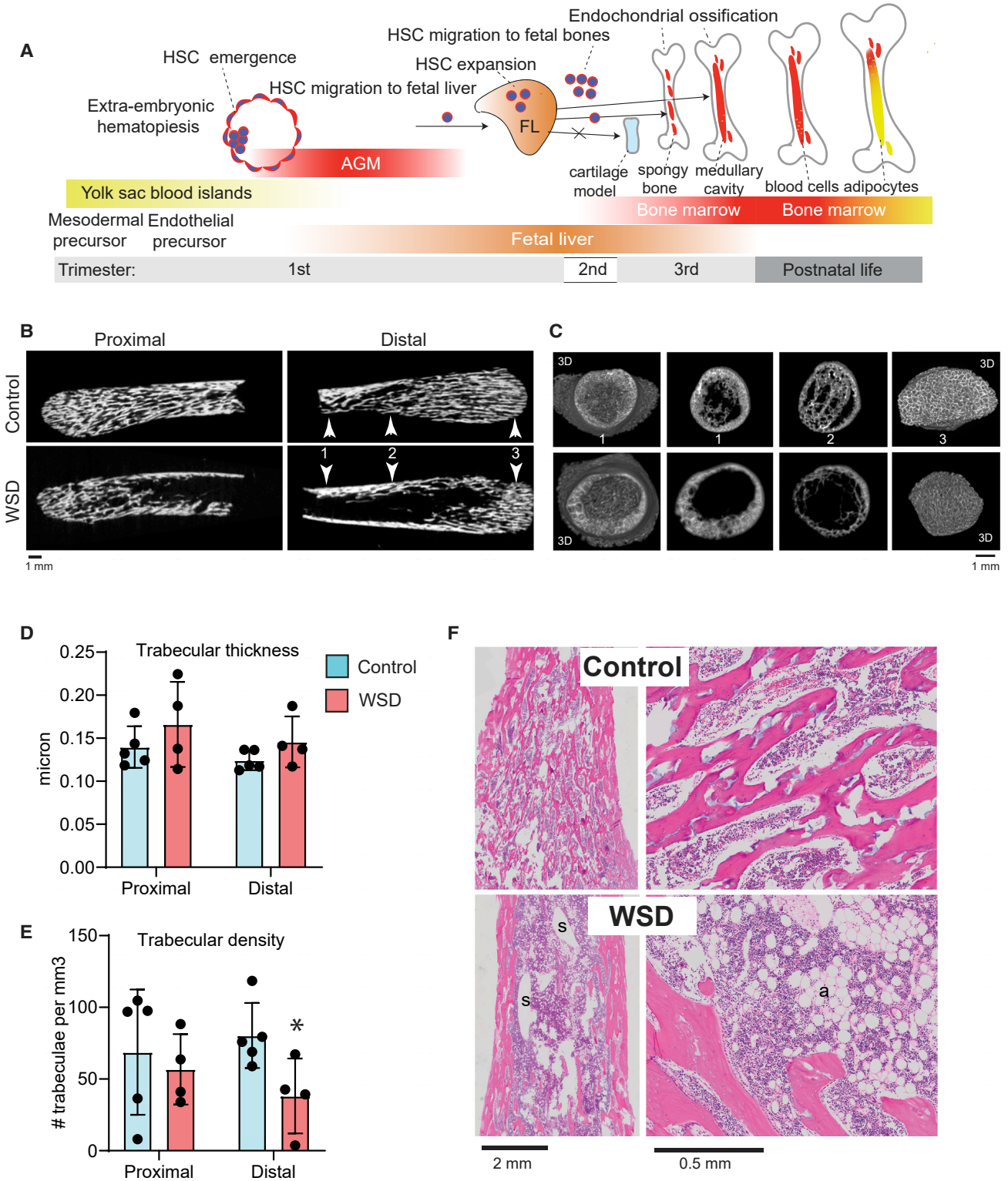


**Figure 1. Maternal WSD induces FBM adipogenesis**

(A) Migration of HSPCs between hematopoietic sites during development. Human HSPCs emerge in the aorta-gonad-mesonephros (AGM) during the first trimester (embryonic day 26 [E26]–E40), and fetal liver (FL) colonization starts at E28. During the second and third

*(legend continued on next page)*

potential risk of pre-term birth associated with consumption of a WSD (Frias et al., 2011; Roberts et al., 2021; Salati et al., 2019), fetuses were collected at gestational day (GD) 130–135 (term 165 ± 10 days). Here, we report for the first time that the chronic consumption of a maternal WSD leads to remodeling of the transcriptional landscape of FBM HSPCs in rhesus macaques.

## RESULTS

### The impact of maternal WSD on fetal development

Dams consuming the WSD exhibited a significantly higher percentage of total body fat before pregnancy and greater body weights during pregnancy than control dams (Figures S1A–S1C; Table S1). Pregnancy rates were not significantly different between the two groups (Table S2). While fetal weights were not significantly affected by maternal WSD, fetal retroperitoneal fat pad weight and maternal and umbilical artery glucose levels were significantly elevated in the WSD group (Figures S1D–S1G; Table S1). Fetal weight was significantly correlated with maternal weight at the Cesarean (C)-section but not with paternal weight or parental age (Table S3). To elucidate the effects of maternal WSD on FBM development (Figure 1A), we performed microcomputed tomography (microCT) and histological analyses of fetal femurs. Femurs of both control and WSD fetuses were highly trabeculated (Figures 1B and 1C). While the average trabecular thickness in fetal femurs was not significantly different between the WSD and control groups, the trabecular thickness in the distal femur was positively correlated with maternal glucose levels at the time of C-section (Figure 1D; Table S3). Additionally, trabecular density was significantly reduced in the distal femurs of WSD fetuses (Figure 1E). The BM of fetal femurs derived from the WSD group were densely populated with adipocytes, while the femurs of control fetuses only occasionally contained adipocytes (Figure 1F). We next performed quantitative immunohistochemical analysis of fetal sterna, representing an alternative site of hematopoiesis. Maternal WSD induced a significant increase in the number of adipocytes in fetal sterna, while adipocytes were only occasionally detected in control sterna (Figures S2A and S2B). The total number of macrophages and HSPCs per sternal section was not significantly different between the control and WSD groups. However, a significantly higher proportion of macrophages and HSPCs was found in close proximity to FBM adipocytes in the sterna of WSD fetuses compared with controls (Figures S2C–S2H). These data demonstrate that maternal WSD induces FBM adiposity in fetal bones.

### Characterization of rhesus macaque fetal HSPCs at single-cell resolution

We next determined the transcriptional landscape of FBM HSPCs at single-cell resolution. HSPCs were isolated from the long bones of control and WSD-exposed fetuses using nonhuman primate (NHP)-specific anti-CD34 antibodies before being profiled by droplet-based single-cell RNA sequencing (scRNA-seq) (Figures S1A and S3A). Dimension reduction and clustering of $CD34^+$ scRNA profiles revealed that the transcriptomes of HSPCs from control and WSD-exposed fetuses were largely overlapping (Figure S3B), with a total of 21 cell clusters identified (Table S4). Consolidation of redundant clusters resulted in fewer hematopoietic progenitor clusters organized in a continuum state (Figure 2A). These clusters were annotated based on markers highly expressed in each cluster relative to the remaining clusters (Table S4). This approach allowed us to identify a cluster of hematopoietic stem cells (HSCs) expressing high levels of *HOXA9* and *HOPX*; proliferating HSCs marked by high *MKI67* expression levels (Miller et al., 2018); megakaryocytic-erythroid progenitors (MEPs) expressing *KLF1* and *HBA*; common lymphoid progenitors (CLPs) expressing *IL7R*, *RAG1*, and *DNTT*; pre-conventional dendritic cell (cDC) precursors expressing *CCR2*, *MAMU-DRA*, and *CD74*; pre-plasmacytoid DCs (pDCs) expressing *IRF7* and *CCL3*; granulocyte-myeloid progenitors (GMPs) expressing *ELANE* and *MPO*; common monocyte progenitors (cMoPs) expressing *OAZ1* and *LYZ*; and promonocytes expressing myeloid cell markers *S100A8*, *IL1B*, and *VCAN* (Asplund et al., 2010, 2011; Chang et al., 2012; Kapellos et al., 2019) (Figures 2B–2D and S3C;

trimesters, HSPCs migrate from the FL to the fetal bone marrow (FBM). BM adipogenesis begins during postnatal life and is associated with the formation of the central medullary cavity.

(B) Representative longitudinal midline cross-sections across the bone shafts of the proximal and distal femurs of control and WSD fetuses. Arrowheads and numbers point at the location of radial cross-sections shown in (C).

(C) Radial cross-sections across the distal femurs. Far-left and far-right images represent the three-dimensional (3D) view of the femurs, looking from open and closed ends, respectively. Middle panels (positions 1 and 2) represent the view of the 1-mm-thick slices across fetal femurs.

(D and E) Mean trabecular thickness (D) and connectivity density (E) across the proximal and distal femur. Bars are means ± SEM; data points represent biological replicates (5 control fetuses and 4 WSD fetuses); unpaired t tests; *$p < 0.05$.

(F) Representative images of H&E-stained proximal femurs from the control and WSD fetuses; a, adipocytes; s, sinusoids.

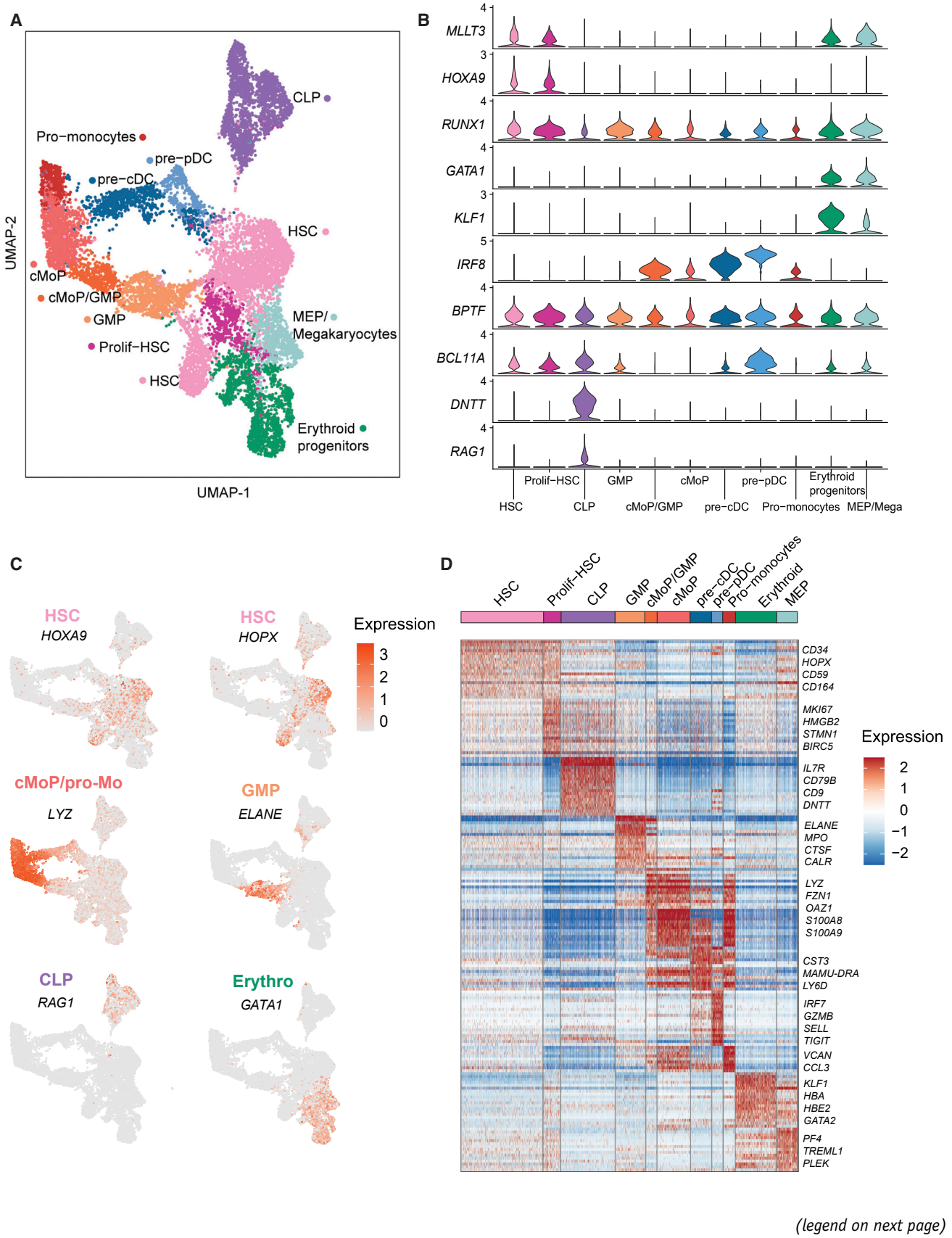


*(legend on next page)*

Table S4). Furthermore, as observed in fetal human HSCs, fetal macaque HSCs showed high expression levels of the transcription factor *MLLT3* gene, the master regulator of human HSC maintenance (Calvanese et al., 2019). Additionally, fetal rhesus macaque HSCs expressed high levels of *CD164*, encoding the sialomucin adhesive glycoprotein, expressed in the most primitive branches of human $CD34^+$ HSPCs (Pellin et al., 2019). Fetal macaque HSCs also expressed *HOXA9*, the master transcriptional regulator of HSC differentiation (Lebert-Ghali et al., 2016; Sugimura et al., 2017), as well as *RUNX1,* encoding the essential transcription factor required for HSC maintenance (Jacob et al., 2010) (Figures 2B–2D and S3C). We also confirmed that rhesus macaque and human (Ranzoni et al., 2021) fetal HSPCs share lineage-specific genes expressed in megakaryocyte-erythroid progenitors (*GATA1/2*, *PLEK*, *KLF1*, *MS4A2*, and *BLVRB*), granulocyte-monocyte progenitors (*AZU1*, *LYZ*, and *MPO*), DC progenitors (*IRF8*), and lymphoid progenitors (*HMGB2* and *CD79B*) (Figures 2B–2D and S3C; Table S4). *CD38* was broadly expressed in fetal HSPCs (Figure S3C), consistent with a previous study, suggesting an overlap in transcriptional states between $CD34^+$ $CD38^-$ and $CD34^+CD38^+$ human HSPCs (Pellin et al., 2019). Furthermore, CLPs formed a distinct cell cluster and exhibited a unique gene-expression pattern characterized by high expression of *DNTT* and *RAG1* (Figures 2B, 2C, and S3C; Table S4). The CLP cluster was further subdivided into CLP-1 (expressing the T cell marker *CD3D*), CLP-2 (expressing the B cell markers *CD79B* and *MAMU-DRA*), and proliferating CLPs (expressing high levels of *MKI67*) (Figures 4C and S3C). These data demonstrate that the single-cell transcriptome of rhesus macaque FBM HSPCs exhibits significant similarities with human fetal HSPCs.

## Maternal WSD induces a proinflammatory phenotype in fetal HSPCs and macrophages

The analysis of differentially expressed genes (DEGs) within HSCs revealed that maternal WSD exposure leads to upregulation of pathways associated with myeloid cell activation, including NOD-like receptor (NLR), Toll-like receptor (TLR), and tumor necrosis factor α (TNF-α) signaling pathways in FBM HSCs (Figure 3A). Moreover, the proinflammatory genes *S100A8/9*, *NFKB1A*, and *PTGS2* were highly upregulated in both HSCs and cMoPs (Table S5). As described for sternal macrophages, long-bone macrophage frequencies were not affected by maternal WSD (Figure 3B). However, FBM macrophages from the WSD group produced significantly higher levels of TNF-α than those from the control group following stimulation with the synthetic triacylated lipopeptide Pam3CysSerLys4 (Pam3CSK4, a TLR1/2 ligand) (Figures 3C and 3D). Moreover, the magnitude of the TNF-α response to Pam3CSK4 by FBM macrophages positively correlated with maternal body fat measured prior to pregnancy (Figure 3E). The frequencies of myeloid subsets residing in fetal blood and FL were not affected by maternal WSD exposure (Figures S4A–S4E). Collectively, these data demonstrate that a maternal WSD exposure results in heightened proinflammatory responses by FBM macrophages.

## Maternal WSD attenuates B cell development in fetal bones

Flow cytometry analysis of $CD34^-CD45^+$ immune cells showed that maternal WSD significantly reduced B cell content in the FBM. In contrast, proportions of FBM $CD3^+$ T lymphocytes that mature in the thymus and can subsequently be recruited into the BM (Comazzetto et al., 2021) were not significantly different between the two groups (Figures 4A and 4B). The frequencies of lymphoid subsets residing in fetal blood and FL were not significantly affected by maternal WSD (Figures S4A–S4E). The analysis of DEGs in fetal CLPs and HSCs revealed a significant decrease in the expression of several transcriptional regulators (*BCL11A*, *BTG2*, *HHEX*, *BPTF*, *NCL*, and *MLLT3*) and cell adhesion molecules (*CD164*, *ITGA4*, *ESAM*, and *CD37*) in WSD-exposed fetuses (Figures 4C and 4D; Table S5). The *MLLT3* (Calvanese et al., 2019) and *CD164* (Pellin et al., 2019) genes have been previously shown to be essential for the maintenance and the hematopoietic reconstitution ability of HSPCs. The most prominent downregulated genes included *BTK,* required for pre-B cell differentiation (Xu et al., 2007), and *ERG,* which is essential for lymphopoiesis (Bergiers et al., 2018; Ng et al., 2020; Sugimura et al., 2017), as well as genes involved in the lymphoid differentiation pathway (*ETV6*, *SMARCB1*, *GRB2*, *SYK*, and *TXNDC12*) (Table S5). Furthermore, we detected significant downregulation of *BCL11A*, required for fetal hematopoiesis (Ding et al., 2021), *IRF3*, the lymphoid transcription factor involved in the interferon signaling pathway (Au et al., 1998), and *CD164* and *ITGA4* (which were also downregulated in HSCs), as well as *CD79A*, *VPREB1*, *RAG1*, and *HMGB2*, which play a critical role in

**Figure 2. Single-cell transcriptome of FBM HSPCs**

(A) Uniform manifold approximation and projection (UMAP) representation of single-cell clusters after dimension reduction of sorted $CD34^+$ HSPCs. Progenitor names are indicated.

(B) Expression levels of transcriptional regulators of HSPC differentiation identified in the present study.

(C) Expression levels of key lineage-specific markers (gene names are shown in black) in HSPCs; progenitor names are color coded.

(D) Heatmap of progenitor cluster-specific genes; only a subset of lineage-specific genes is shown.

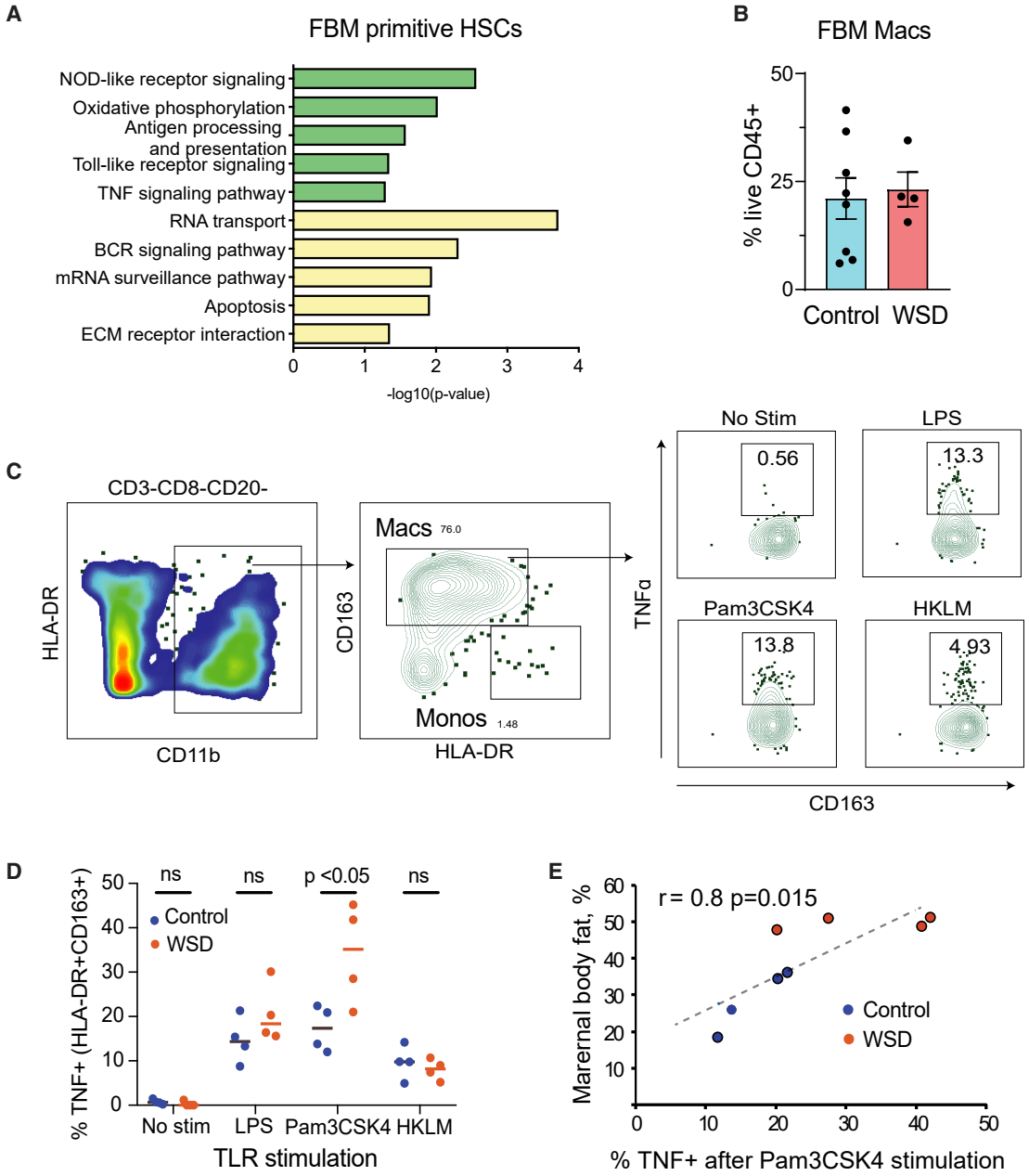


**Figure 3. Maternal WSD induces a hyperinflammatory phenotype in FBM progenitors**

(A) Pathway analysis of differentially expressed genes in primitive CD34$^+$ HSCs in response to maternal WSD; green, upregulated genes; yellow, downregulated genes.

(B) Macrophage frequencies in the tibial FBM of control and WSD fetuses; data points represent biological replicates (8 control fetuses and 4 WSD fetuses); bars are means ± SEM.

(C) Gating strategy used for studying Toll-like receptor ligand responses in FBM macrophages; macrophages (Macs) and monocytes (Monos) were identified within the Lin$^-$CD11b$^+$ myeloid cell population; frequencies of TNF-$\alpha^+$CD163$^+$ macrophages without simulation or in the presence of indicated ligands are indicated.

(D) TNF-$\alpha$ responses in FBM macrophages following TLR ligand stimulation; each data point shows the percentage of TNF-$\alpha^+$ cells within the CD11b$^+$HLA-DR$^+$CD163$^+$ gate; data points represent biological replicates (n = 4 control fetuses and 4 WSD fetuses); horizontal bars are group means. All two-group comparisons were tested for statistical differences using an unpaired t test.

(E) Correlation between maternal body fat before pregnancy and macrophage responses to Pam3CSK4 stimulation; Pearson coefficient (r) and p values are indicated.

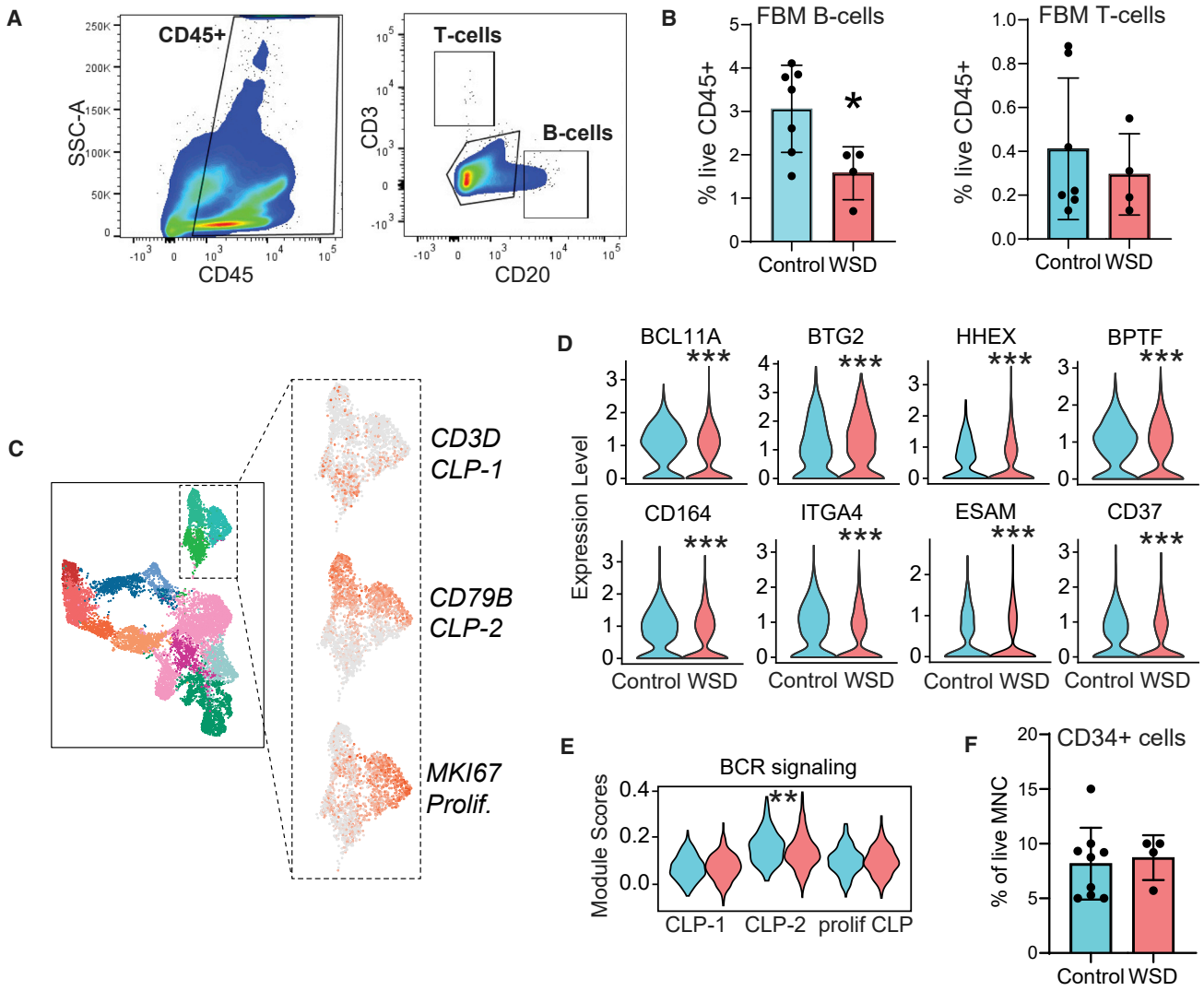


**Figure 4. Maternal WSD attenuates fetal B cell development in long bones**

(A) Gating strategy used for identifying FBM $CD3^+$ T cells and $CD20^+$ B cells within the parental $CD45^+$ gate.

(B) B cell and T cell frequencies in the $CD34^-CD45^+$ fraction of the FBM; data points represent biological replicates (7 control fetuses and 4 WSD fetuses). Bars are means ± SEM. All two-group comparisons were tested for statistical differences using an unpaired t test; *$p < 0.05$.

(C) The spatial positions and expression of specific genes in CLP subtypes.

(D) Normalized RNA levels of transcriptional regulators (top row) and adhesion molecules (bottom row) downregulated (***$p < 0.001$) in fetal CLPs with a maternal WSD.

(E) Violin plot comparing module scores for B cell receptor (BCR) signaling within the CLP clusters. Group differences in gene expression were tested for statistical significance using a nonparametric Wilcoxon's rank-sum test in Seurat, as described in the experimental procedures; **$p < 0.01$.

(F) Fetal $CD34^+$ cell frequencies in FBM; $CD34^+$ cells were isolated from the tibial mononuclear cell (MNC) fraction using the anti-CD34 antibody. Each data point represents a percentage of $CD34^+$ cells within live FBM MNCs (9 control fetuses and 4 WSD fetuses).

lymphoid lineage development in human fetuses (Ranzoni et al., 2021) (Figure 4D; Table S5). The DEG analysis revealed a suppression of B cell receptor signaling in B cell progenitors (CLP-2) with maternal WSD (Figures 4C and 4E). However, the proportions of $CD34^+$ HSPCs within the mononuclear FBM fraction were not significantly different between the two groups (Figure 4F; Table S6). Collectively, our analyses indicate that a maternal WSD changes the transcriptional program of FBM CLPs, potentially dysregulating B cell development.

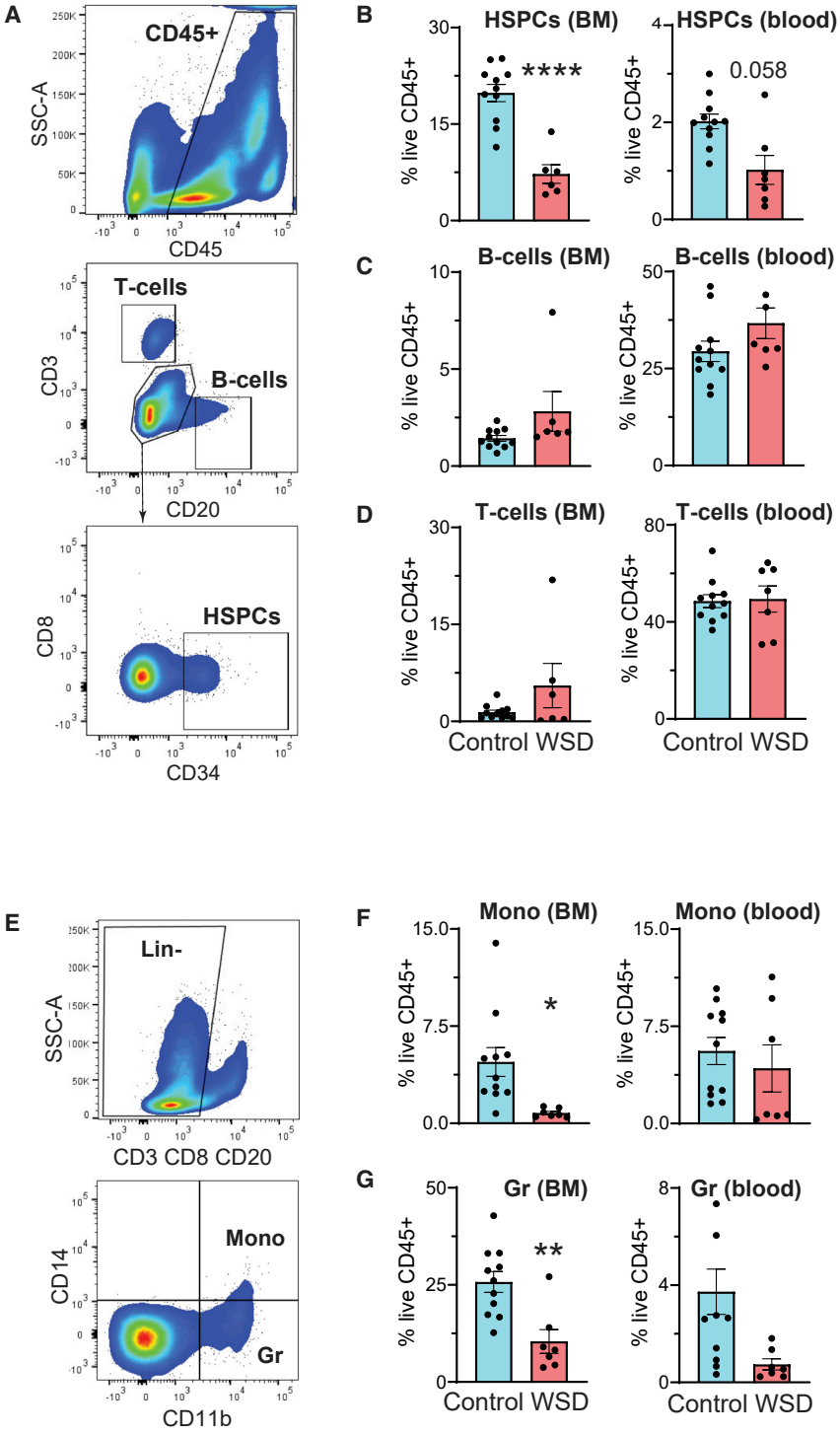


**Figure 5. Maternal WSD reduces the engraftment ability of FBM HSPCs**

(A) Gating strategy used for the analysis of rhesus $CD3^+$ T cells and $CD20^+$ B cells within the $CD45^+$ gate in NSG mice. Rhesus macaque $CD34^+$ HSPCs are identified within the $CD45^+CD3^-CD20^-$ gate.

(B–D) HSPC (B), B cell (C), and T cell (D) frequencies in the $CD45^+$ fraction of the BM and blood of NSG mice.

(E) Gating strategy used for identifying myeloid cells. Rhesus macaque monocytes (Monos) and granulocytes (Grs) are identified within the $Lin^-$ gate as $CD14^+CD11b^+$ or $CD14^-CD11b^+$ cells, respectively.

(F and G) Monocyte (F) and granulocyte (G) frequencies in the BM and blood of NSG mice. FBM $CD34^+$ HSPCs were isolated from 2 control and 2 WSD fetal donors and injected into 5–6 NSG mice per donor. Data points represent immune cell frequencies detected in successfully engrafted NSG mice; bars are means ± SEM; unpaired t tests, *$p < 0.05$, **$p < 0.01$, ****$p < 0.0001$.

## Maternal WSD alters the engraftment ability of FBM HSPCs under regenerative stress

To test whether maternal WSD alters HSPC function *in vivo*, we transplanted 120,000 tibial FBM $CD34^+$ HSPCs into nonlethally irradiated immunodeficient NOD/SCID/*IL2rγ*$^{-/-}$ (NSG) mice (Figures S4F and S4G). Thirteen weeks following engraftment, the levels of macaque $CD34^+$ cells in the BM were significantly lower in the mice engrafted with HSPCs from the WSD group compared with those engrafted with control HSPCs (Figures 5A and 5B). We

observed no significant group differences in frequencies of B and T cells in the BM and blood of NSG mice (Figures 5C and 5D). In contrast, frequencies of myeloid cells, including monocytes, and granulocytes (gating strategy developed by Radtke et al., 2019) were significantly reduced in the BM of NSG mice that received $CD34^+$ cells from maternal WSD fetuses (Figures 5E–5G). To test whether a maternal WSD alters the differentiation of FBM HSPCs, we isolated engrafted $CD34^+$ cells from the BM of NSG mice and conducted a colony-forming assay (CFU) using 250 $CD34^+$ cells, derived from the control and WSD groups. There were no significant group differences in the number of granulocyte-macrophage progenitor colony-forming units (CFU-GMs) or erythroid burst-forming units (BFU-Es) (Figure S4H), suggesting that control and WSD HSPCs exhibit similar *in vitro* erythro-myeloid differentiation abilities. In summary, our results demonstrate that maternal WSD changes the intrinsic properties of FBM HSPCs, thus affecting their engraftment in the BM under regenerative conditions.

## DISCUSSION

Maternal obesity adversely impacts immune function in the offspring; however, the underlying mechanisms remain largely unknown. Experimental and clinical obesity in adults has been linked to the dysregulation of hematopoiesis (Liu et al., 2018; Singer et al., 2014; van den Berg et al., 2016), mediated in part via gut-derived microbial-derived metabolites and TLR ligands (Yan et al., 2018). Previous studies have also shown that maternal WSD compromises FL hematopoiesis (Kamimae-Lanning et al., 2015), but very little is known about the effect of WSD on developmental hematopoiesis during fetal life in models that resemble human development. Here, we demonstrate that NHP hematopoietic markers share lineage-specific genes closely aligned with those of humans and explore the potential effects of a maternal WSD on macaque FBM HSPCs.

In the present study, we found that maternal WSD exposure triggers premature FBM adipogenesis. The presence of adipocytes in the BM cavity is associated with a postnatal state, as reported by previous NHP (Robino et al., 2020), rodent, and human (Rosen et al., 2009; Scheller et al., 2015) studies. The pattern of fetal BM adipogenesis induced by a maternal WSD also resembles age- and obesity-related replacement of hematopoietic marrow with adipogenic marrow in adults (Adler et al., 2014; Ambrosi et al., 2017; Li et al., 2018; Scheller et al., 2015). BM adipocytes have been initially described as negative regulators of hematopoiesis under regenerative stress in mice (Naveiras et al., 2009). These findings are also consistent with our transplantation data showing that maternal WSD has a negative impact on HSPC engraftment. We also demonstrated that maternal WSD evokes a persistent inflammatory gene signature in FBM HSPCs and a latent hyperinflammatory phenotype in FBM macrophages. These findings suggest that a maternal WSD *in utero* regulates fetal immune system development, in part, through reprogramming fetal HSPC function. Given the negative effects of maternal WSD on hematopoietic function in long bones in NHP fetuses, alongside increased adipocyte content, we speculate that excess BM adiposity *in utero* has a negative effect on specific aspects of hematopoiesis. However, it is possible that other components of the FBM niche (such as stromal and bone cells) are also affected by a maternal WSD, and more study is necessary to understand how alterations in the cross-talk between an adipocyte-rich microenvironment and HSPCs affect the subsequent development and function of the immune system. For example, we have previously shown that adult macaque BM adipose tissue releases factors enriched in extracellular vesicles (Robino et al., 2020), representing the potential regulators of HSPC function and differentiation (Butler et al., 2018; Hornick et al., 2016; Huan et al., 2015). Likewise, there may be metabolic signals from the maternal microbiome that play a role in prenatal dietary priming of hematopoietic progenitors and contribute to developmental programming (Kalbermatter et al., 2021).

Our immunophenotypic analysis shows that a maternal WSD also reduced FBM B cell numbers, while our scRNA-Seq analysis revealed that maternal WSD reduced the expression of B cell development genes in FBM CLPs. We also demonstrate that FBM HSPCs from the WSD group exhibited reduced engraftment and myeloid lineage reconstitution abilities in nonobese recipient mice, which is consistent with our scRNA-seq data showing that maternal WSD results in downregulation of cell adhesion molecules in FBM HSPCs. These data are consistent with the concept that maternal WSD drives intrinsic changes in HSPCs that affect their biological function in the FBM. We did not observe significant effects of maternal WSD on myeloid cell numbers in fetal bones, FL, or peripheral blood. In addition, a previous study in mice has shown that in the FL, maternal obesity, together with a maternal high-fat diet, skewed HSPCs toward a myeloid-biased differentiation that was niche dependent (Kamimae-Lanning et al., 2015). Furthermore, our studies show that WSD enhanced TLR1/2 cytokine responses by FBM macrophages, which is consistent with rodent studies that demonstrated hyperinflammatory responses in BM-derived macrophages (Friedman et al., 2018) and microglia (Edlow et al., 2019) of offspring born to dams on a high-fat diet, and with our scRNA-seq analysis showing the upregulation of TLR and TNF-$\alpha$ signaling pathways and proinflammatory genes in monocyte progenitors from WSD fetuses. Our study

therefore expands on previous reports that obesity drives peripheral adipose tissue inflammation (McNelis and Olefsky, 2014; Reilly and Saltiel, 2017; Russo et al., 2020; Singer et al., 2015) and suggests that diet-induced expansion of BM adipose tissue is also associated with an increase in a proinflammatory environment in the FBM.

Our study has several limitations. The small sample size might limit our power to detect smaller effects caused by maternal WSD on fetal outcomes. Nevertheless, the number of biological replicates (n = 2–3 per group) used in our scRNA-seq study is consistent with previous scRNA-seq studies of human HSPCs using two stem cell donors (Crosse et al., 2020; Pellin et al., 2019; Velten et al., 2017). The small number of fetuses in the WSD group precluded an examination of sex differences in maternal effects on fetal hematopoiesis. While small effects of a maternal WSD on fetal bone trabecular development were detected, further studies are needed to understand the impact of maternal diet on fetal bone development in NHPs. In summary, this study sets the stage for understanding the link between maternal obesity, prenatal nutrition, and diseases involving immune progeny of the HSPC compartment in children (Friedman, 2018; Jonscher et al., 2020; Netea et al., 2020) and highlights the need to better understand the susceptibility of the developing a hematopoietic system to metabolic dysregulation over lifetime.

## EXPERIMENTAL PROCEDURES

### Resource availability

#### *Corresponding author*

Further information and requests for resources and reagents should be directed to the corresponding author, Oleg Varlamov (varlamov@ohsu.edu).

#### *Materials availability*

This study did not generate new unique reagents.

### Dietary intervention

All animal procedures were approved by the Oregon National Primate Research Center (ONPRC) Institutional Animal Care and Use Committee and comply with the Animal Welfare Act and the APA Guidelines for Ethical Conduct in the Care and Use of Nonhuman Animals in Research. Dietary interventions and animal care have been previously described (Bishop et al., 2018a, 2021; True et al., 2017; Varlamov et al., 2017). The control diet (Purina Lab Diet fiber-balanced monkey chow no. 5000; Purina Mills, St. Louis, MO, USA) contains 15% calories from fat, 27% from protein, and 58% from carbohydrates. The WSD diet (Purina 5LOP, Purina Mills) contains 36% calories from fat, 18% from protein, and 46% from carbohydrates.

### Animal breeding and C-section

The animal cohort described in the present study underwent two fertility trials, after 3.5 (Bishop et al., 2018b) and 5.5 (present study) years of treatment. Fertility trial procedures were previously described (Bishop et al., 2018b). Briefly, pregnancies were initiated by timed mating breeding utilizing proven male breeders maintained on a control diet. To minimize the potential effects of paternal weight and age differences on fetal development, one male breeder whose age and weight were two standard deviations lower than the group average and maternal and fetal analyses associated with this breeder were not included in this study. Male breeders used in the study (n = 9) ranged in age from 12 to 18.8 years and in weight from 11 to 14.7 kg. Females used in this study (n = 9 control animals; n = 4 WSD animals) ranged in age from 7.8 to 8.9 years and in weight from 5.9 to 10.8 kg. Nine control and 4 WSD fetuses were used in this study.

### Fetal necropsy

Fetal morphometric parameters and whole-body weights were recorded. Terminal blood was collected from the abdominal aorta or caudal vena cava. The thoracic cavity was opened, and all tissues and organs were examined for normal fetal development *in situ*. Fetal organs were collected, and their weights were recorded (Table S1). The middle portion of the FL that encompasses the gallbladder was dissected, perfused with Belzer UW Cold Storage Solution (Bridge to Life, Northbrook, IL, USA), and shipped on ice to University of Colorado for the flow cytometry analysis of FL immune cells. Fetal femurs, tibias, and sternum were collected and processed within 15–30 min of exsanguination.

### Cell isolation from the FBM and FL

Both fetal tibias were completely cleaned of all soft and cartilaginous tissues, placed in a ceramic mortar containing 20 mL ice-cold *X-Vivo* media (Lonza, Basel, Switzerland), cut into smaller fragments, and manually crushed with a ceramic pestle. The cell suspension and bone fragments were transferred into a 30 μm nylon cell strainer (Thermo Fisher Scientific, Waltham, MA, USA) and rinsed with 10 mL ice-cold *X-Vivo* media (Lonza). Cell filtrate was subjected to centrifugation at room temperature for 30 min at 400 × *g* on a Ficoll gradient (Stem Cell Technologies, Vancouver, BC, Canada). FBM mononuclear cells residing at the interface of *X-Vivo* media and Ficoll were carefully collected, and red blood cells were lysed for 8 min using the RBC lysis buffer ( Stem Cell Technologies). Cells were washed three times with PBS, and $CD34^+$ cells were isolated as described (Robino et al., 2020) using rhesus macaque-specific antibodies to CD34 (clone 563; BD Pharmingen, San Jose, CA, USA) and the anti-PE MACS magnetic bead system (Miltenyi Biotec, Bergisch Gladbach, Germany) with the supplied reagents. $CD34^+$ HSPC and $CD34^-$ flow-through cell fractions were cryopreserved using CryoStor CS10 (STEMCELL Technologies).

### Engraftment of FBM HSPCs in NSG mice

Engraftments were performed on 4-week-old female NSG mice (Jackson Laboratory, Bar Harbor, ME, USA; strain: 005557 NOD.Cg-Prkdc Il2rg/SzJ) of at least 15 g body weight. The NSG mice were maintained on regular rodent chow under a sterile environment. To minimize nonhematopoietic toxicity, a nonlethal dose of 200 cGy was administered to NSG mice. Cryopreserved FBM $CD34^+$ cells derived from two control and two WSD macaque

fetuses were thawed, washed with *X-Vivo* media (Lonza), counted, and kept on ice before injection. 5–6 NSG mice were injected with 120,000 $CD34^+$ cells derived from each donor, as described below. Two negative control mice were injected with the *X-Vivo* media. Blood collection was performed once a month. All 11 mice injected with $CD34^+$ cells from the control fetuses survived the postengraftment period. Five out of 11 mice injected with $CD34^+$ cells from the WSD fetuses died prior to engraftment. All mice were euthanized 13 weeks after injection. Both mouse tibias were cleaned of soft tissues, cut at the proximal and distal ends, and flashed with 1 mL ice-cold 2 mM EDTA-PBS. Blood and BM samples (Table S6) were analyzed.

### Flow cytometry

Cryopreserved cells, including tibial $CD34^-$ FBM and peripheral blood mononuclear cells (PBMCs), were analyzed by flow cytometry using monoclonal antibodies validated for binding to rhesus macaque proteins (Burwitz et al., 2014). FBM cells ($5 \times 10^5$) were stimulated with LPS (TLR4 agonist 1 μg/mL), Pam3CSK4 (TLR1/2 agonist, 1 μg/mL), or HKLM (TLR2 agonist, $10^8$ particles/mL) for 8 h in the presence of 5 μg/mL brefeldin A (Sigma-Aldrich). TLR agonists were purchased from InvivoGen (San Diego, CA, USA). Cells were stained with antibodies to CD11b, HLA-DR, and CD163 to delineate monocytes/macrophages. Following surface staining, cells were permeabilized and stained with monoclonal antibodies to TNF-α (clone MAb11, Invitrogen). Samples were washed in fluorescence-activated cell sorting (FACS) buffer and analyzed on an LSRII flow cytometer. Data were analyzed using FlowJo v.10 (Tree Star, Ashland, OR, USA) and Prism v.6 (GraphPad Software, San Diego, CA, USA).

### FACS sorting and scRNA-seq of fetal $CD34^+$ cells

Freshly thawed antibody-labeled $CD34^+$ HSPCs were enriched for live cells by FACS using SYTOX Blue dead cell stain (Thermo Fisher Scientific) on a BD FACS Aria Fusion cell sorter. Cells were sorted into RPMI containing 30% FBS, 5% glutamine, and antibiotics. Samples from each group were sorted into one single tube. Cells from each group were then counted in triplicates on a TC20 Automated Cell Counter (Bio-Rad), washed, and resuspended in 1× PBS with 0.04% BSA to a final concentration of 1,200 cells/μL. Single-cell suspensions were then immediately loaded on a 10x Genomics Chromium Controller with a loading target of 17,600 cells. Libraries were generated using the 3′ V3 chemistry per the manufacturer's instructions (10x Genomics, Pleasanton, CA, USA) and sequenced on an Illumina NovaSeq with a sequencing target of 30,000 reads per cell.

### scRNA-seq data analysis

Raw reads were aligned and quantified using the Cell Ranger's *count* function (v.4.0, 10x Genomics) against the *Macaca mulatta* reference genome (MMul10) using the STAR aligner. Downstream processing of aligned reads was performed using Seurat (v.3.2.2). Droplets with ambient RNA or poor-quality cells (cells with fewer than 400 detected genes), potential doublets (cells with more than 4,000 detected genes), and dying cells (cells with more than 20% total mitochondrial gene expression) were excluded during the initial quality control. To rule out biases in different stages of cell cycle, cells were then scored for S or G2/M phase using a catalog of canonical markers (Kowalczyk et al., 2015). Cells with high ribosomal gene expression (≥30 pc of total gene expression) were further excluded before integration. Data objects from the two groups were integrated using Seurat's *IntegrateData* function (Stuart et al., 2019). Data normalization and variance stabilization were performed using the *SCTransform* function using a regularized negative binomial regression to correct for differential effects of mitochondrial and ribosomal gene-expression profiles. Dimension reduction was performed using the *RunPCA* function to obtain the first 30 principal components followed by clustering using the *FindClusters* function in Seurat. Clusters were visualized using uniform manifold approximation and projection (UMAP) algorithm as implemented by Seurat's *runUMAP* function. Cell types were assigned to individual clusters using *FindMarkers* function with a fold change cutoff of at least 0.4 and using a known catalog of well-characterized scRNA markers for HSCs (Table S5) (Pellin et al., 2019). Differential expression analysis of the chow and WSD groups within each cell type was performed using the nonparametric Wilcoxon rank-sum test in Seurat. Genes with at least a 0.4-fold change ($\log_2$ scale) and with an adjusted p value ≤0.05 were considered significant. Pathway analysis of differential signatures was performed using Enrichr (https://maayanlab.cloud/Enrichr/). For module scoring, we compared gene signatures and pathways from KEGG (https://www.genome.jp/kegg/pathway.html) in subpopulations using Seurat's *AddModuleScore* function. Group differences were compared using unpaired t test followed by Welch's correction.

### Statistical analyses

A correlation analysis between maternal/paternal and fetal parameters was conducted by calculating the Pearson correlation coefficients and their associated p values. The p values were then adjusted using the Benjamini-Hochberg procedure to control the false discovery rate (FDR) below 0.05 for selected physiological parameters. This method was implemented in R using the "p.adjust" function. All two-group comparisons were tested for statistical differences using unpaired t tests.

## DATA AND CODE AVAILABILITY

The accession number for the NCBI SRA gene expression data reported in this paper is PRJNA723061.

## SUPPLEMENTAL INFORMATION

Supplemental information can be found online at https://doi.org/10.1016/j.stemcr.2022.10.003.

## AUTHOR CONTRIBUTIONS

scRNA-seq assay and bioinformatic analysis were generated by S.S. Immunohistochemistry was conducted by C.N.C. and L.K.P. HSPC transplantation in NSG mice were performed by O.V., J.J.R., and D.G. Immunophenotyping experiments were performed by B.J.B., S.S., O.V., M.J.N., and J.J.R. Flow cytometry data were analyzed by I.M., O.V., S.S., D.G., M.J.N., E.M.P., and B.J.B. Fetal tissue collection was performed by D.T., J.J.R., and O.V. Statistical

analysis was performed by O.V., S.S., B.J.B., X.J., and W.S. MicroCT analysis was done by J.R.L. and W.P. The manuscript was written by O.V., S.S., and I.M. O.V., J.D.H., M.J.N., J.E.F., S.R.W., and C.T.R. contributed to concept development, provided access to samples, and edited the manuscript.

## ACKNOWLEDGMENTS

We thank Dr. Lauren Drew Martin for help with blood collections, Kati Marshall for help in animal handling and transplantation, Dr. Jennifer Atwood for assistance with cell sorting, and Dr. Melanie Oakes for assistance with library preparation and sequencing of 10x samples. This study was supported by NIH grants P50 HD071836 to C.T.R. and J.D.H., P51 OD01192 for operation of the ONPRC, 1R01AI142841 and 1R01AI145910 to I.M., R24-DK090964 to J.E.F., F30-DK122672 to M.J.N., R01-DK108910 to S.R.W., R01-DK119394 to E.M.P., and the shared instrumentation grant 1S10OD025002-01.

## CONFLICTS OF INTEREST

The authors declare no competing interests.

Received: March 17, 2022
Revised: October 4, 2022
Accepted: October 5, 2022
Published: November 3, 2022

## REFERENCES

Adler, B.J., Kaushansky, K., and Rubin, C.T. (2014). Obesity-driven disruption of haematopoiesis and the bone marrow niche. Nat. Rev. Endocrinol. *10*, 737–748. https://doi.org/10.1038/nrendo.2014.169.

Ambrosi, T.H., Scialdone, A., Graja, A., Gohlke, S., Jank, A.M., Bocian, C., Woelk, L., Fan, H., Logan, D.W., Schürmann, A., et al. (2017). Adipocyte accumulation in the bone marrow during obesity and aging impairs stem cell-based hematopoietic and bone regeneration. Cell Stem Cell *20*, 771–784.e6. https://doi.org/10.1016/j.stem.2017.02.009.

Asplund, A., Fridén, V., Stillemark-Billton, P., Camejo, G., and Bondjers, G. (2011). Macrophages exposed to hypoxia secrete proteoglycans for which LDL has higher affinity. Atherosclerosis *215*, 77–81. https://doi.org/10.1016/j.atherosclerosis.2010.12.017.

Asplund, A., Stillemark-Billton, P., Larsson, E., Rydberg, E.K., Moses, J., Hultén, L.M., Fagerberg, B., Camejo, G., and Bondjers, G. (2010). Hypoxic regulation of secreted proteoglycans in macrophages. Glycobiology *20*, 33–40. https://doi.org/10.1093/glycob/cwp139.

Au, W.C., Moore, P.A., LaFleur, D.W., Tombal, B., and Pitha, P.M. (1998). Characterization of the interferon regulatory factor-7 and its potential role in the transcription activation of interferon A genes. J. Biol. Chem. *273*, 29210–29217. https://doi.org/10.1074/jbc.273.44.29210.

Batchelder, C.A., Duru, N., Lee, C.I., Baker, C.A.R., Swainson, L., McCune, J.M., and Tarantal, A.F. (2014). Myeloid-lymphoid ontogeny in the rhesus monkey (Macaca mulatta). Anat. Rec. *297*, 1392–1406. https://doi.org/10.1002/ar.22943.

Bergiers, I., Andrews, T., Vargel Bölükbaşı, Ö., Buness, A., Janosz, E., Lopez-Anguita, N., Ganter, K., Kosim, K., Celen, C., Itır Perçin, G., et al. (2018). Single-cell transcriptomics reveals a new dynamical function of transcription factors during embryonic hematopoiesis. Elife *7*, e29312. https://doi.org/10.7554/eLife.29312.

Bishop, C.V., Mishler, E.C., Takahashi, D.L., Reiter, T.E., Bond, K.R., True, C.A., Slayden, O.D., and Stouffer, R.L. (2018a). Chronic hyperandrogenemia in the presence and absence of a western-style diet impairs ovarian and uterine structure/function in young adult rhesus monkeys. Hum. Reprod. *33*, 128–139. https://doi.org/10.1093/humrep/dex338.

Bishop, C.V., Stouffer, R.L., Takahashi, D.L., Mishler, E.C., Wilcox, M.C., Slayden, O.D., and True, C.A. (2018b). Chronic hyperandrogenemia and western-style diet beginning at puberty reduces fertility and increases metabolic dysfunction during pregnancy in young adult, female macaques. Hum. Reprod. *33*, 694–705. https://doi.org/10.1093/humrep/dey013.

Bishop, C.V., Takahashi, D., Mishler, E., Slayden, O.D., Roberts, C.T., Hennebold, J., and True, C. (2021). Individual and combined effects of 5-year exposure to hyperandrogenemia and Western-style diet on metabolism and reproduction in female rhesus macaques. Hum. Reprod. *36*, 444–454. https://doi.org/10.1093/humrep/deaa321.

Bowie, M.B., Kent, D.G., Dykstra, B., McKnight, K.D., McCaffrey, L., Hoodless, P.A., and Eaves, C.J. (2007). Identification of a new intrinsically timed developmental checkpoint that reprograms key hematopoietic stem cell properties. Proc. Natl. Acad. Sci. USA *104*, 5878–5882. https://doi.org/10.1073/pnas.0700460104.

Burwitz, B.J., Reed, J.S., Hammond, K.B., Ohme, M.A., Planer, S.L., Legasse, A.W., Ericsen, A.J., Richter, Y., Golomb, G., and Sacha, J.B. (2014). Technical advance: liposomal alendronate depletes monocytes and macrophages in the nonhuman primate model of human disease. J. Leukoc. Biol. *96*, 491–501. https://doi.org/10.1189/jlb.5TA0713-373R.

Butler, J.T., Abdelhamed, S., and Kurre, P. (2018). Extracellular vesicles in the hematopoietic microenvironment. Haematologica *103*, 382–394. https://doi.org/10.3324/haematol.2017.183335.

Calvanese, V., Nguyen, A.T., Bolan, T.J., Vavilina, A., Su, T., Lee, L.K., Wang, Y., Lay, F.D., Magnusson, M., Crooks, G.M., et al. (2019). MLLT3 governs human haematopoietic stem-cell self-renewal and engraftment. Nature *576*, 281–286. https://doi.org/10.1038/s41586-019-1790-2.

Chang, M.Y., Chan, C.K., Braun, K.R., Green, P.S., O'Brien, K.D., Chait, A., Day, A.J., and Wight, T.N. (2012). Monocyte-to-macrophage differentiation: synthesis and secretion of a complex extracellular matrix. J. Biol. Chem. *287*, 14122–14135. https://doi.org/10.1074/jbc.M111.324988.

Christensen, J.L., Wright, D.E., Wagers, A.J., and Weissman, I.L. (2004). Circulation and chemotaxis of fetal hematopoietic stem cells. PLoS Biol. *2*, E75. https://doi.org/10.1371/journal.pbio.0020075.

Comazzetto, S., Shen, B., and Morrison, S.J. (2021). Niches that regulate stem cells and hematopoiesis in adult bone marrow. Dev. Cell *56*, 1848–1860. https://doi.org/10.1016/j.devcel.2021.05.018.

Coşkun, S., Chao, H., Vasavada, H., Heydari, K., Gonzales, N., Zhou, X., de Crombrugghe, B., and Hirschi, K.K. (2014). Development of the fetal bone marrow niche and regulation of HSC quiescence and homing ability by emerging osteolineage cells. Cell Rep. *9*, 581–590. https://doi.org/10.1016/j.celrep.2014.09.013.

Crosse, E.I., Gordon-Keylock, S., Rybtsov, S., Binagui-Casas, A., Felchle, H., Nnadi, N.C., Kirschner, K., Chandra, T., Tamagno, S., Webb, D.J., et al. (2020). Multi-layered spatial transcriptomics identify secretory factors promoting human hematopoietic stem cell development. Cell Stem Cell *27*, 822–839.e8. https://doi.org/10.1016/j.stem.2020.08.004.

Ding, Y., Wang, W., Ma, D., Liang, G., Kang, Z., Xue, Y., Zhang, Y., Wang, L., Heng, J., Zhang, Y., and Liu, F. (2021). Smarca5-mediated epigenetic programming facilitates fetal HSPC development in vertebrates. Blood *137*, 190–202. https://doi.org/10.1182/blood.2020005219.

Edlow, A.G., Glass, R.M., Smith, C.J., Tran, P.K., James, K., and Bilbo, S. (2019). Placental macrophages: a window into fetal microglial function in maternal obesity. Int. J. Dev. Neurosci. *77*, 60–68. https://doi.org/10.1016/j.ijdevneu.2018.11.004.

Frias, A.E., Morgan, T.K., Evans, A.E., Rasanen, J., Oh, K.Y., Thornburg, K.L., and Grove, K.L. (2011). Maternal high-fat diet disturbs uteroplacental hemodynamics and increases the frequency of stillbirth in a nonhuman primate model of excess nutrition. Endocrinology *152*, 2456–2464. https://doi.org/10.1210/en.2010-1332.

Friedman, J.E. (2018). Developmental programming of obesity and diabetes in mouse, monkey, and man in 2018: where are we headed? Diabetes *67*, 2137–2151. https://doi.org/10.2337/dbi17-0011.

Friedman, J.E., Dobrinskikh, E., Alfonso-Garcia, A., Fast, A., Janssen, R.C., Soderborg, T.K., Anderson, A.L., Reisz, J.A., D'Alessandro, A., Frank, D.N., et al. (2018). Pyrroloquinoline quinone prevents developmental programming of microbial dysbiosis and macrophage polarization to attenuate liver fibrosis in offspring of obese mice. Hepatol. Commun. *2*, 313–328. https://doi.org/10.1002/hep4.1139.

Gao, X., Xu, C., Asada, N., and Frenette, P.S. (2018). The Hematopoietic Stem Cell Niche: From Embryo to Adult. Development *145*. https://doi.org/10.1242/dev.139691.

Gomez Perdiguero, E., Klapproth, K., Schulz, C., Busch, K., Azzoni, E., Crozet, L., Garner, H., Trouillet, C., de Bruijn, M.F., Geissmann, F., and Rodewald, H.R. (2015). Tissue-resident macrophages originate from yolk-sac-derived erythro-myeloid progenitors. Nature *518*, 547–551. https://doi.org/10.1038/nature13989.

Hornick, N.I., Doron, B., Abdelhamed, S., Huan, J., Harrington, C.A., Shen, R., Cambronne, X.A., Chakkaramakkil Verghese, S., and Kurre, P. (2016). AML suppresses hematopoiesis by releasing exosomes that contain microRNAs targeting c-MYB. Sci. Signal. *9*, ra88. https://doi.org/10.1126/scisignal.aaf2797.

Huan, J., Hornick, N.I., Goloviznina, N.A., Kamimae-Lanning, A.N., David, L.L., Wilmarth, P.A., Mori, T., Chevillet, J.R., Narla, A., Roberts, C.T., Jr., et al. (2015). Coordinate regulation of residual bone marrow function by paracrine trafficking of AML exosomes. Leukemia *29*, 2285–2295. https://doi.org/10.1038/leu.2015.163.

Jacob, B., Osato, M., Yamashita, N., Wang, C.Q., Taniuchi, I., Littman, D.R., Asou, N., and Ito, Y. (2010). Stem cell exhaustion due to Runx1 deficiency is prevented by Evi5 activation in leukemogenesis. Blood *115*, 1610–1620. https://doi.org/10.1182/blood-2009-07-232249.

Jonscher, K.R., Abrams, J., and Friedman, J.E. (2020). Maternal diet alters trained immunity in the pathogenesis of pediatric NAFLD. J. Cell. Immunol. *2*, 315–325. https://doi.org/10.33696/immunology.2.061.

Kalbermatter, C., Fernandez Trigo, N., Christensen, S., and Ganal-Vonarburg, S.C. (2021). Maternal microbiota, early life colonization and breast milk drive immune development in the newborn. Front. Immunol. *12*, 683022. https://doi.org/10.3389/fimmu.2021.683022.

Kamimae-Lanning, A.N., Krasnow, S.M., Goloviznina, N.A., Zhu, X., Roth-Carter, Q.R., Levasseur, P.R., Jeng, S., McWeeney, S.K., Kurre, P., and Marks, D.L. (2015). Maternal high-fat diet and obesity compromise fetal hematopoiesis. Mol. Metab. *4*, 25–38. https://doi.org/10.1016/j.molmet.2014.11.001.

Kapellos, T.S., Bonaguro, L., Gemünd, I., Reusch, N., Saglam, A., Hinkley, E.R., and Schultze, J.L. (2019). Human monocyte subsets and phenotypes in major chronic inflammatory diseases. Front. Immunol. *10*, 2035. https://doi.org/10.3389/fimmu.2019.02035.

Kim, S., Kim, N., Presson, A.P., Metzger, M.E., Bonifacino, A.C., Sehl, M., Chow, S.A., Crooks, G.M., Dunbar, C.E., An, D.S., et al. (2014). Dynamics of HSPC repopulation in nonhuman primates revealed by a decade-long clonal-tracking study. Cell Stem Cell *14*, 473–485. https://doi.org/10.1016/j.stem.2013.12.012.

Kowalczyk, M.S., Tirosh, I., Heckl, D., Rao, T.N., Dixit, A., Haas, B.J., Schneider, R.K., Wagers, A.J., Ebert, B.L., and Regev, A. (2015). Single-cell RNA-seq reveals changes in cell cycle and differentiation programs upon aging of hematopoietic stem cells. Genome Res. *25*, 1860–1872. https://doi.org/10.1101/gr.192237.115.

Larochelle, A., Savona, M., Wiggins, M., Anderson, S., Ichwan, B., Keyvanfar, K., Morrison, S.J., and Dunbar, C.E. (2011). Human and rhesus macaque hematopoietic stem cells cannot be purified based only on SLAM family markers. Blood *117*, 1550–1554. https://doi.org/10.1182/blood-2009-03-212803.

Lebert-Ghali, C.É., Fournier, M., Kettyle, L., Thompson, A., Sauvageau, G., and Bijl, J.J. (2016). Hoxa cluster genes determine the proliferative activity of adult mouse hematopoietic stem and progenitor cells. Blood *127*, 87–90. https://doi.org/10.1182/blood-2015-02-626390.

Lee, C.C.I., Fletcher, M.D., and Tarantal, A.F. (2005). Effect of age on the frequency, cell cycle, and lineage maturation of rhesus monkey (Macaca mulatta) CD34+ and hematopoietic progenitor cells. Pediatr. Res. *58*, 315–322. https://doi.org/10.1203/01.PDR.0000169975.30339.32.

Li, Z., Hardij, J., Bagchi, D.P., Scheller, E.L., and MacDougald, O.A. (2018). Development, regulation, metabolism and function of bone marrow adipose tissues. Bone *110*, 134–140. https://doi.org/10.1016/j.bone.2018.01.008.

Liu, A., Chen, M., Kumar, R., Stefanovic-Racic, M., O'Doherty, R.M., Ding, Y., Jahnen-Dechent, W., and Borghesi, L. (2018). Bone marrow lympho-myeloid malfunction in obesity requires precursor cell-autonomous TLR4. Nat. Commun. *9*, 708. https://doi.org/10.1038/s41467-018-03145-8.

McGrath, K.E., Frame, J.M., and Palis, J. (2015). Early hematopoiesis and macrophage development. Semin. Immunol. *27*, 379–387. https://doi.org/10.1016/j.smim.2016.03.013.

McNelis, J.C., and Olefsky, J.M. (2014). Macrophages, immunity, and metabolic disease. Immunity *41*, 36–48. https://doi.org/10.1016/j.immuni.2014.05.010.

Messaoudi, I., Estep, R., Robinson, B., and Wong, S.W. (2011). Nonhuman primate models of human immunology. Antioxid. Redox Signal. *14*, 261–273. https://doi.org/10.1089/ars.2010.3241.

Miller, I., Min, M., Yang, C., Tian, C., Gookin, S., Carter, D., and Spencer, S.L. (2018). Ki67 is a graded rather than a binary marker of proliferation versus quiescence. Cell Rep. *24*, 1105–1112.e5. https://doi.org/10.1016/j.celrep.2018.06.110.

Morrison, S.J., Hemmati, H.D., Wandycz, A.M., and Weissman, I.L. (1995). The purification and characterization of fetal liver hematopoietic stem cells. Proc. Natl. Acad. Sci. USA *92*, 10302–10306. https://doi.org/10.1073/pnas.92.22.10302.

Naveiras, O., Nardi, V., Wenzel, P.L., Hauschka, P.V., Fahey, F., and Daley, G.Q. (2009). Bone-marrow adipocytes as negative regulators of the haematopoietic microenvironment. Nature *460*, 259–263. https://doi.org/10.1038/nature08099.

Netea, M.G., Domínguez-Andrés, J., Barreiro, L.B., Chavakis, T., Divangahi, M., Fuchs, E., Joosten, L.A.B., van der Meer, J.W.M., Mhlanga, M.M., Mulder, W.J.M., et al. (2020). Defining trained immunity and its role in health and disease. Nat. Rev. Immunol. *20*, 375–388. https://doi.org/10.1038/s41577-020-0285-6.

Ng, A.P., Coughlan, H.D., Hediyeh-Zadeh, S., Behrens, K., Johanson, T.M., Low, M.S.Y., Bell, C.C., Gilan, O., Chan, Y.C., Kueh, A.J., et al. (2020). An Erg-driven transcriptional program controls B cell lymphopoiesis. Nat. Commun. *11*, 3013. https://doi.org/10.1038/s41467-020-16828-y.

Odaka, Y., Nakano, M., Tanaka, T., Kaburagi, T., Yoshino, H., Sato-Mito, N., and Sato, K. (2010). The influence of a high-fat dietary environment in the fetal period on postnatal metabolic and immune function. Obesity *18*, 1688–1694. https://doi.org/10.1038/oby.2009.513.

Orkin, S.H., and Zon, L.I. (2008). Hematopoiesis: an evolving paradigm for stem cell biology. Cell *132*, 631–644. https://doi.org/10.1016/j.cell.2008.01.025.

Pellin, D., Loperfido, M., Baricordi, C., Wolock, S.L., Montepeloso, A., Weinberg, O.K., Biffi, A., Klein, A.M., and Biasco, L. (2019). A comprehensive single cell transcriptional landscape of human hematopoietic progenitors. Nat. Commun. *10*, 2395. https://doi.org/10.1038/s41467-019-10291-0.

Radtke, S., Chan, Y.Y., Sippel, T.R., Kiem, H.P., and Rongvaux, A. (2019). MISTRG mice support engraftment and assessment of nonhuman primate hematopoietic stem and progenitor cells. Exp. Hematol. *70*, 31–41.e1. https://doi.org/10.1016/j.exphem.2018.12.003.

Ranzoni, A.M., Tangherloni, A., Berest, I., Riva, S.G., Myers, B., Strzelecka, P.M., Xu, J., Panada, E., Mohorianu, I., Zaugg, J.B., and Cvejic, A. (2021). Integrative single-cell RNA-seq and ATAC-seq analysis of human developmental hematopoiesis. Cell Stem Cell *28*, 472–487.e7. https://doi.org/10.1016/j.stem.2020.11.015.

Rastogi, S., Rojas, M., Rastogi, D., and Haberman, S. (2015). Neonatal morbidities among full-term infants born to obese mothers. J. Matern. Fetal Neonatal Med. *28*, 829–835. https://doi.org/10.3109/14767058.2014.935324.

Reilly, S.M., and Saltiel, A.R. (2017). Adapting to obesity with adipose tissue inflammation. Nat. Rev. Endocrinol. *13*, 633–643. https://doi.org/10.1038/nrendo.2017.90.

Roberts, V.H.J., Streblow, A.D., Gaffney, J.E., Rettke, S.P., Frias, A.E., and Slayden, O.D. (2021). Placental glucose uptake in a nonhuman primate model of western-style diet consumption and chronic hyperandrogenemia exposure. Reprod. Sci. *28*, 2574–2581. https://doi.org/10.1007/s43032-021-00526-1.

Robino, J.J., Pamir, N., Rosario, S., Crawford, L.B., Burwitz, B.J., Roberts, C.T., Jr., Kurre, P., and Varlamov, O. (2020). Spatial and biochemical interactions between bone marrow adipose tissue and hematopoietic stem and progenitor cells in rhesus macaques. Bone *133*, 115248. https://doi.org/10.1016/j.bone.2020.115248.

Rosen, C.J., Ackert-Bicknell, C., Rodriguez, J.P., and Pino, A.M. (2009). Marrow fat and the bone microenvironment: developmental, functional, and pathological implications. Crit. Rev. Eukaryot. Gene Expr. *19*, 109–124.

Russo, L., Muir, L., Geletka, L., Delproposto, J., Baker, N., Flesher, C., O'Rourke, R., and Lumeng, C.N. (2020). Cholesterol 25-hydroxylase (CH25H) as a promoter of adipose tissue inflammation in obesity and diabetes. Mol. Metab. *39*, 100983. https://doi.org/10.1016/j.molmet.2020.100983.

Salati, J.A., Roberts, V.H.J., Schabel, M.C., Lo, J.O., Kroenke, C.D., Lewandowski, K.S., Lindner, J.R., Grove, K.L., and Frias, A.E. (2019). Maternal high-fat diet reversal improves placental hemodynamics in a nonhuman primate model of diet-induced obesity. Int. J. Obes. *43*, 906–916. https://doi.org/10.1038/s41366-018-0145-7.

Scheller, E.L., Doucette, C.R., Learman, B.S., Cawthorn, W.P., Khandaker, S., Schell, B., Wu, B., Ding, S.Y., Bredella, M.A., Fazeli, P.K., et al. (2015). Region-specific variation in the properties of skeletal adipocytes reveals regulated and constitutive marrow adipose tissues. Nat. Commun. *6*, 7808. https://doi.org/10.1038/ncomms8808.

Singer, K., DelProposto, J., Morris, D.L., Zamarron, B., Mergian, T., Maley, N., Cho, K.W., Geletka, L., Subbaiah, P., Muir, L., et al. (2014). Diet-induced obesity promotes myelopoiesis in hematopoietic stem cells. Mol. Metab. *3*, 664–675. https://doi.org/10.1016/j.molmet.2014.06.005.

Singer, K., Maley, N., Mergian, T., DelProposto, J., Cho, K.W., Zamarron, B.F., Martinez-Santibanez, G., Geletka, L., Muir, L., Wachowiak, P., et al. (2015). Differences in hematopoietic stem cells contribute to sexually dimorphic inflammatory responses to high fat diet-induced obesity. J. Biol. Chem. *290*, 13250–13262. https://doi.org/10.1074/jbc.M114.634568.

Stuart, T., Butler, A., Hoffman, P., Hafemeister, C., Papalexi, E., Mauck, W.M., 3rd, Hao, Y., Stoeckius, M., Smibert, P., and Satija, R. (2019). Comprehensive integration of single-cell data. Cell *177*, 1888–1902.e21. https://doi.org/10.1016/j.cell.2019.05.031.

Sugimura, R., Jha, D.K., Han, A., Soria-Valles, C., da Rocha, E.L., Lu, Y.F., Goettel, J.A., Serrao, E., Rowe, R.G., Malleshaiah, M., et al.

(2017). Haematopoietic stem and progenitor cells from human pluripotent stem cells. Nature *545*, 432–438. https://doi.org/10.1038/nature22370.

Suk, D., Kwak, T., Khawar, N., Vanhorn, S., Salafia, C.M., Gudavalli, M.B., and Narula, P. (2016). Increasing maternal body mass index during pregnancy increases neonatal intensive care unit admission in near and full-term infants. J. Matern. Fetal Neonatal Med. *29*, 3249–3253. https://doi.org/10.3109/14767058.2015.1124082.

Sykes, S.M., and Scadden, D.T. (2013). Modeling human hematopoietic stem cell biology in the mouse. Semin. Hematol. *50*, 92–100. https://doi.org/10.1053/j.seminhematol.2013.03.029.

Tarantal, A.F., Hartigan-O'Connor, D.J., and Noctor, S.C. (2022). Translational utility of the nonhuman primate model. Biol. Psychiatry. Cogn. Neurosci. Neuroimaging *7*, 491–497. https://doi.org/10.1016/j.bpsc.2022.03.001.

True, C.A., Takahashi, D.L., Burns, S.E., Mishler, E.C., Bond, K.R., Wilcox, M.C., Calhoun, A.R., Bader, L.A., Dean, T.A., Ryan, N.D., et al. (2017). Chronic combined hyperandrogenemia and western-style diet in young female rhesus macaques causes greater metabolic impairments compared to either treatment alone. Hum. Reprod. *32*, 1880–1891. https://doi.org/10.1093/humrep/dex246.

van den Berg, S.M., Seijkens, T.T.P., Kusters, P.J.H., Beckers, L., den Toom, M., Smeets, E., Levels, J., de Winther, M.P.J., and Lutgens, E. (2016). Diet-induced obesity in mice diminishes hematopoietic stem and progenitor cells in the bone marrow. FASEB J *30*, 1779–1788. https://doi.org/10.1096/fj.201500175.

Varlamov, O., Bishop, C.V., Handu, M., Takahashi, D., Srinivasan, S., White, A., and Roberts, C.T., Jr. (2017). Combined androgen excess and Western-style diet accelerates adipose tissue dysfunction in young adult, female nonhuman primates. Hum. Reprod. *32*, 1892–1902. https://doi.org/10.1093/humrep/dex244.

Varlamov, O., Bucher, M., Myatt, L., Newman, N., and Grant, K.A. (2020). Daily ethanol drinking followed by an abstinence period impairs bone marrow niche and mitochondrial function of hematopoietic stem/progenitor cells in rhesus macaques. Alcohol Clin. Exp. Res. *44*, 1088–1098. https://doi.org/10.1111/acer.14328.

Velten, L., Haas, S.F., Raffel, S., Blaszkiewicz, S., Islam, S., Hennig, B.P., Hirche, C., Lutz, C., Buss, E.C., Nowak, D., et al. (2017). Human haematopoietic stem cell lineage commitment is a continuous process. Nat. Cell Biol. *19*, 271–281. https://doi.org/10.1038/ncb3493.

Wu, C., Espinoza, D.A., Koelle, S.J., Potter, E.L., Lu, R., Li, B., Yang, D., Fan, X., Donahue, R.E., Roederer, M., and Dunbar, C.E. (2018). Geographic clonal tracking in macaques provides insights into HSPC migration and differentiation. J. Exp. Med. *215*, 217–232. https://doi.org/10.1084/jem.20171341.

Xu, S., Lee, K.G., Huo, J., Kurosaki, T., and Lam, K.P. (2007). Combined deficiencies in Bruton tyrosine kinase and phospholipase Cgamma2 arrest B-cell development at a pre-BCR+ stage. Blood *109*, 3377–3384. https://doi.org/10.1182/blood-2006-07-036418.

Yan, H., Baldridge, M.T., and King, K.Y. (2018). Hematopoiesis and the bacterial microbiome. Blood *132*, 559–564. https://doi.org/10.1182/blood-2018-02-832519.